Non-random island nucleation in the electrochemical roughening on Pt(111)

Rost, M.J.; Jacobse, L.; Koper, M.T.M.

How to cite: *Angew. Chem. Int. Ed.* **2023**, *62*, e202216376
doi.org/10.1002/anie.202216376

Electrochemistry

Non-Random Island Nucleation in the Electrochemical Roughening on Pt(111)

Marcel J. Rost, Leon Jacobse, and Marc T. M. Koper*

Abstract: Many chemical surface systems develop ordered nano-islands during repeated reaction and restoration. Platinum is used in electrochemical energy applications, like fuel cells and electrolysers, although it is scarce, expensive, and degrades. During oxidation-reduction cycles, simulating device operation, nucleation and growth of nano-islands occurs that eventually enhances the dissolution. Preventing nucleation would be the most effective solution. However, little is known about the atomic details of the nucleation; a process almost impossible to observe. Here, we analyze the nuclei-distance distribution mapping out the underlying atomic mechanism: a rarely observed, non-random nucleation takes place. Special, preferential nucleation sites that *a priori* do not exist, develop initially via a precursor and eventually form a semi-ordered Pt-oxide structure. This precursor mechanism seems to be general, possibly explaining also the nano-island formation on other surfaces/reactions.

1. Introduction

The statistical nature of most deposition techniques leads to a random distribution of arriving atoms or molecules (flux).[1–4] At low enough temperatures, where the diffusion is kinetically hindered, each arriving atom serves as a nucleus site leading to a random lateral distribution. At higher temperatures, thus active diffusion, adatoms diffuse towards the steps in order to compensate the enhanced chemical potential setup by the deposition flux of arriving-atoms that naturally exceeds the equilibrium chemical potential on the terraces given by the local equilibrium adatom pressure. The latter is determined by the Boltzmann-distribution and Gibbs–Thomson relation, taking into account the adatom formation energy, temperature, and local step curvature.[5–7] However, depending on the ratio of flux/mobility (F/M) in combination with the distance towards the nearest step, adatoms do not only have the chance to meet each other during their statistical dance, but also to linger a while as a cluster and collect enough other adatoms to overcome the nucleation barrier by forming a stable island with the critical nucleus size. This leads to a *quasi random* lateral distribution of nuclei, if one considers homoepitaxial systems without preferential nucleation sites, in contrast to e.g. the elbows of the well-known herringbone reconstruction on Au(111) that are often used to create nano-patterned structures.[8] As a next refinement, one can consider also ripening effects, where atoms are transported between nucleated islands under attachment/detachment-limited or diffusion-limited conditions (Ostwald ripening) as well as the migration/diffusion of (small) islands as a whole (Smoluchowski ripening).[9,10] These different mechanisms obviously alter the lateral distribution of nuclei leading to a deviation from the quasi random lateral distribution. With the above insight, it becomes clear that a properly chosen statistical function of the lateral nuclei distribution should be able to distinguish different underlying atomic processes even though they are not directly observed.

This very fundamental and interesting aspect has been theoretically addressed for the diffusion-zone model already by Lewis and Campbell in 1967,[11] derived from rate equations for nucleation & growth by Venables in 1973,[12] and followed up by Metois in 1976.[13] The correlations between the nuclei are measured with the radial distribution function, which is a normalized isotropic pair correlation function (PCF), also called the island-island distance distribution function. For a 2D lattice with N nuclei,

$$\int_{r=0}^{\infty} \rho g(r) 2\pi r dr = N - 1, \tag{1}$$

in which ρ is nuclei mean density and r the distance from a specific nucleus, the pair correlation function is given by:

$$g(r) = \frac{1}{2\pi r}\frac{1}{N\rho}\left\langle \sum_{i=1}^{N}\sum_{k\neq i}^{N} \delta(r - |r_k - r_i|) \right\rangle. \tag{2}$$

[*] M. J. Rost
Huygens-Kamerlingh Onnes Laboratory, Leiden University
Niels Bohrweg 2, 2333 CA Leiden (The Netherlands)
E-mail: rost@physics.leidenuniv.nl

L. Jacobse
Centre for X-ray and Nano Science CXNS,
Deutsches Elektronen-Synchrotron DESY
Notkestrasse 85, 22607 Hamburg (Germany)

M. T. M. Koper
Leiden Institute of Chemistry, Leiden University
Einsteinweg 55, 2333 CC Leiden (The Netherlands)

Figure 1 sketches inherent differences in $g(r)$ for the different active atomic mechanisms: hit & stick nucleation, capture zone vs. rate equation diffusion, and repulsive interaction.

Note the significantly different shape of $g(r)$ in Figure 1d with a peak clearly above the average nuclei density and oscillations, which origin is manifested either in the nucleation on pre-existing, preferential sites or the existence of a repulsive interaction. Such systems have been noticed since the '60s,[14–17] and addressed in the review by Evans.[18]

The electrochemical roughening on Pt(111) under Oxidation-Reduction-Cycles (ORCs) serves as an ideal model system for the understanding of platinum electrode degradation and dissolution in electrochemical energy conversion systems, as nano-islands nucleate and grow.[19,20] The general growth mechanism has been understood on an atomic scale and can be described analytically by a combined homoepitaxial growth mode of adatom as well as vacancy "mound formation", leading to a satisfactory agreement (and prediction) with experiments.[21] Due to the increased size of platinum oxide, stress is built up and atoms are pushed into a higher level (in the end even on top of the surface) during the oxidation. As the oxygen atoms are leaving during the reduction, vacancies and holes are formed in the surface as well as (ad)atoms on top. Adatom-vacancy annihilation is difficult, because of both the existence of the Ehrlich–Schwoebel barrier,[21] which actually breaks down for small

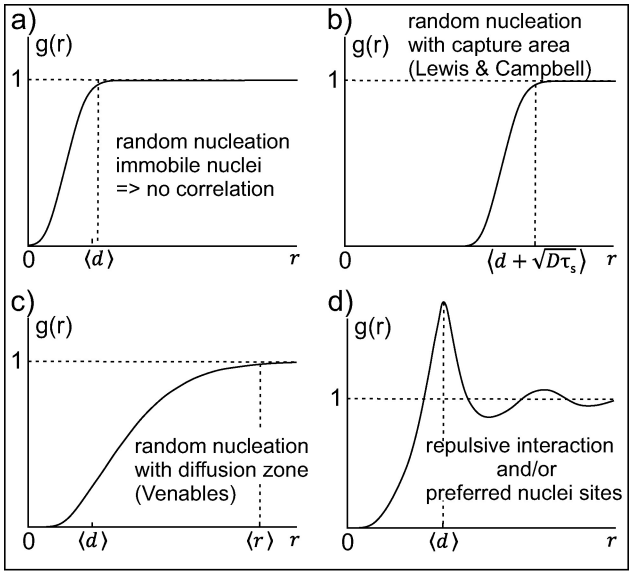

Figure 1. Pair Correlation Function (PCF) $g(r)$: a) in case of a random nucleation with immobile atoms and clusters (hit & stick): the nuclei distance is given by the average nuclei diameter $\langle d \rangle$, b) Lewis & Campbell include a capture area, such that the average nuclei density is reached at larger distances determined by the diffusion constant and time D_{T_s},[11] c) the distribution is further smeared out, when considering rate equations for the nucleation & growth, as Venables did,[12] and d) a significantly different $g(r)$ occurs with oscillations and a peak above 1, if repulsive interactions are present or nucleation occurs on special, preferential sites leading to the nucleation in "unit cells". The Figure is with corrections adapted from Ref. [13].

structures,[22,23] and, therefore probably more dominating, the nucleation of adatoms into stable islands, as they quickly find other ones in their vicinity during their random walk on top of the surface when the oxygen leaves. This leads to an effective flux of both adatoms and vacancies during one ORC enabling the description of the evolution by homoepitaxial crystal growth models.[21]

Although the general growth of the nano-islands is well understood,[21] the early stages, in particular the (pre)nucleation, are surely not. The nucleation starts with a precursor, the so-called place-exchange (PE) process,[24,25] where exactly one adsorbed oxygen atom exchanges its place with one Pt surface atom, lifting the latter up vertically almost a complete step height. We recently provided evidence that 2 oxygen atoms are involved in the formation of one PE atom.[26] Smartly executed in operando Surface X-Ray Diffraction (SXRD) studies have delivered deeper insight,[26–32] as they address the monolayer (ML) percentage of PE atoms as a function of surface/electrode potential, time, charge, and potential sweep rate as well as potential jumps. These experiments confirm not only that the lifted Pt atoms hover "exactly" above their original lattice position,[26,27] that a maximum PE coverage exists up to which the system is fully (structural) reversible and no roughening takes place, that the PE layer can be described best with a 2D random adatom gas model, that nucleation, and thus roughening, takes place when a critical PE coverage is exceeded, but also that there is no lateral ordering of the PE atoms (although 1D chains cannot be ruled out strictly).[26,27] With this insight, one clearly expects a random nucleation and thus a pair correlation function as sketched in Figures 1a–c.

In contrast to the classical PE model, Density Functional Theory (DFT) calculations show stable 1D chains of the PE atoms under electrochemical conditions that order macroscopically in lines or "spoke wheel" structures,[33,34] the latter of which has been observed on Pt(111) in vacuum under high chemical potential (1 to 5 bar oxygen pressure and 400 to 500 K).[35] It is particularly interesting to note here that these chains or spokes are built up structurally from PtO_2 units, the oxide with the lowest formation energy, and that 7 PtO_2 distances (8 Pt atoms in the oxide) equal exactly 8 Pt(111) distances (9 Pt atoms) such that the formation of one line or spoke with this length requires the expulsion of exactly 1 Pt atom. Let us now use the pair correlation function to gain a deeper insight into the nature of the nucleation process.

2. Results and Discussion

Figure 2 shows the early stages during the ORCs, uniquely capturing (almost) all nucleation events. The analyzed data are part of an earlier in operando measurement,[19] in which we correlated the roughness evolution to the electrochemical signal. The complete experimental details are provided in this publication. High resolution Scanning Tunneling Microscope (STM) images that address the transition from slightly dendritic nuclei shapes to more rounded islands

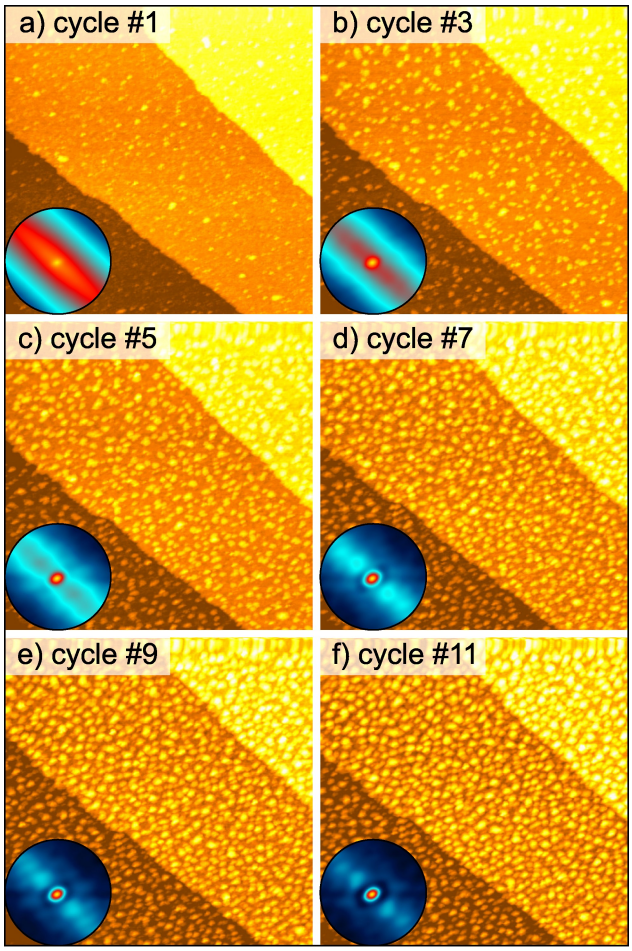

Figure 2. Nucleation events captured with STM images: after a) 1, b) 3, c) 5, d) 7, e) 9, and f) 11 ORCs. The images are 230×230 nm^2 and have been measured with a sample voltage of $U_s = 0.4$ V and a tip voltage $U_t = 0.45$ V (vs. a Reversible Hydrogen Electrode Potential (RHE)) with tunneling currents $I_t < 300$ pA. The images are part of a movie, which can be found as supplementary in Ref. [19] or online Ref. [40]. The insets are corresponding auto-correlations zoomed in to the origin (45 nm). All images have been calculated and displayed with the same contrast and brightness settings as well as amplitude allowing a direct comparison between them. Due to the presence of the steps, a diagonal band is visible in the first correlations. This background band quickly breaks up at the sides and transforms into a hexagonal pattern, due to the island nucleation and growth. The sharpness and intensity becomes more pronounced with increasing ORC.

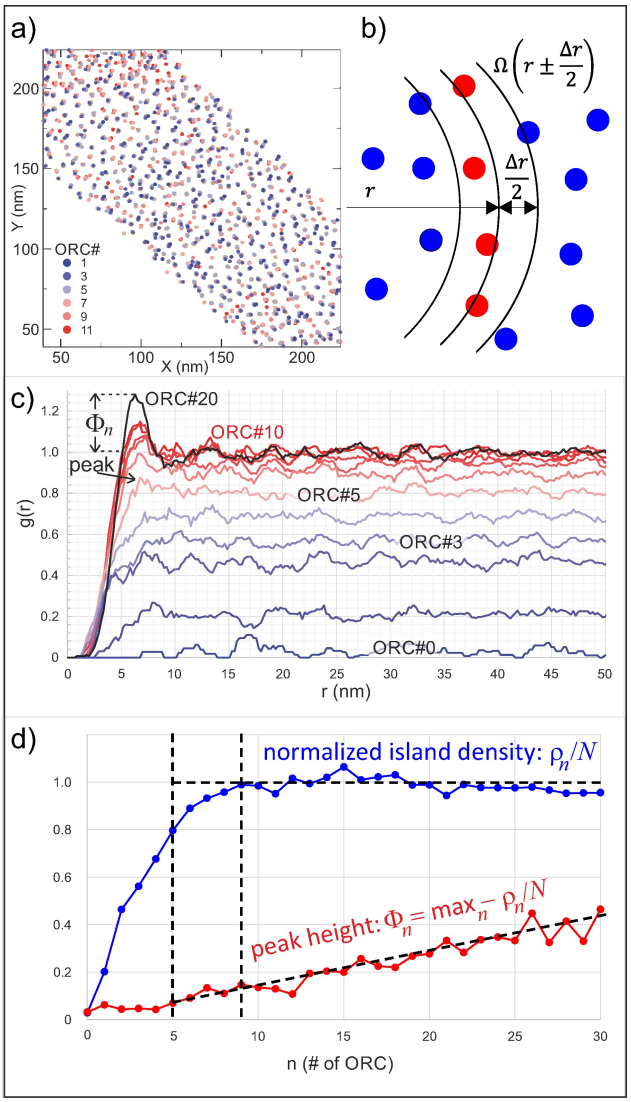

Figure 3. Experimentally determined island-island distribution function: a) map of the island positions of the images shown in Figure 2 for ORC #1, #3, #5, #7, #9, and #11; b) Graphical representation demonstrating the extraction of the data from the measurements, in which we bin all distances within the area Ω; c) Pair Correlation Function for ORCs #0 to #10 plus #20, d) normalized island density (blue) and peak-height evolution (red) as function of ORC number: the peak becomes visible from on ORC#5, which is significantly earlier than ORC#9, at which the maximum island density is reached. We restricted the current analysis, and thus interpretation, up to ORC #20, as there is a transition from 2D to 3D growth at this cycle:[19] the full nucleation density surely has been reached at this stage.

during the early ORCs can be found in Ref. [36]. The results presented here are representative for those obtained from more than forty independent measurements on three different Pt(111) crystals, as illustrated also in the supplementary material in Ref. [37]. Furthermore, the same island size and ordering is also observed in Surface X-ray Diffraction (SXRD) as well as STM measurements from multiple groups.[26,29,30,38,39]

Using a self-programmed, automatic detection Scheme, based on a Laplace filter (second derivative), Figure 3a shows the center positions of the nuclei/islands after cycle 1, 3, 5, 7, 9, and 11 during the sequence of ORCs. We restricted the analysis to one single terrace to prevent non-statistical correlation distances introduced by the presence of the steps. Using the left-to-right and right-to-left measured images, we corrected for piezo hysteresis and creep. The counting mechanism, to extract quantitative values for Equation (2), is shown graphically in Figure 3b, and the final result is shown in Figure 3c.

When comparing our results shown in Figure 3c with the general curves sketched in Figure 1, it is evident that a peak exists that indicates either repulsive interaction between the

depositing atoms or the nucleation at preferential sites. Although the full amplitude of the peak, a measure for the interaction strengths, can only be evaluated at full nucleation density, the peak becomes visible already at 80 % of the full nucleation density ρ, see ORC#5 in Figure 3c. This indicates a rather pronounced repulsive interaction or well-defined preferred nuclei sites and explains also the following surprising observation in the movie,[40] and the images in Figure 2: in the early stages of the evolution it is possible to *guess* where islands will nucleate, although still many islands are missing. Typically the nucleation is a rather instantaneous transition in time during the evolution, as the formed nuclei suck away new arriving material and thus lower the enhanced chemical potential below the nucleation threshold level (otherwise more islands would have nucleated already in the first place). To quantify this effect further, we plot in Figure 3d the actual, normalized, mean island density, ρ_n, in blue and Φ_n in red, which is the maximum density within the first 13 nm minus the actual, mean island density, ρ_n. The full nucleation density is reached at ORC#9 (or even later). In contrast, the peak, Φ, starts rising above the background noise level already at ORC#5, four cycles earlier. It is noteworthy to mention that this rise continues even after the full nucleation has been reached; an observation that has been reported before.[30] What could cause this effect? As a higher peak implies a higher degree of order of the islands, the first, most obvious, mechanism would be enabled material transport between the islands that decreases the remaining statistical variance. This, however, should also lead to coarsening and thus Ostwald ripening, which is not (or only very mildly) observed in all measurements. A second mechanism is naturally manifested in the growth process, which includes an instability (*Zeno-effect*),[21] and drives, therefore, the system to more symmetric and well-defined islands the higher they develop during the ORCs (3D growth). However, this would on the other hand mean that the system is fully developed already in the very early stages (2D), as it is (almost) impossible to move the instability line, the one atomic distance wide groove between two 2D islands, after its creation.[21] A combination of both effects, with limited material transport between the islands, is expected to occur via downhill funneling,[22,23,41,42] allowing for minor movements of the instability lines.

Before concluding our observations and discussing their origin, it is interesting to quantify the nucleus-nucleus distance, and thus the final island size, from these data. The final island radius can be extracted at 50 % of the full nucleation density ρ. With a value of 3.83 nm, the island diameter becomes 7.65 nm and fits nicely with the reported value of 7.2 nm at the same ORC scan-rate using X-Ray measurements.[30] Our earlier reported value of 8.9 nm was derived from Height Difference Correlation Functions (HDCFs).[19] As these functions measure the in-plane travel distance for reaching the maximum height difference, and as this occurs in the corners of the hexagonal unit cell and not at the sides, one needs to divide 8.9 nm by cos(30°) resulting in 7.71 nm, which again is in good agreement with our findings here.

Concluding the observations, it is evident that the nucleation of the nano-islands during the electrochemical roughening of Pt(111) involves either a significant repulsive interaction or the existence of well-ordered preferential nuclei sites. In first instance we can rule out the latter. No reconstruction has been reported on Pt(111) under electrochemical conditions neither by STM nor by SXRD. Moreover, even the sensitive electrochemical fingerprint did not show any hint of a reconstruction, although the reconstructions of Au(100), Au(110), Au(111), Pt(100), and Pt(110) have been easily noticed by this method.[43] In conclusion, there are, *a priori*, no special nuclei sites present, like e.g. in the case of the herringbone reconstruction on Au(111). However, we will remarkably see in the following, that preferential nuclei sites develop on the basis of a repulsive interaction between a precursor of the oxidation during the early stages, and thus not a repulsive interaction between the atoms responsible for the deposition flux: an unexpected fundamental atomic mechanism.

As Pt(111) does not show any reconstruction, special, preferential nuclei sites do not exist *a priori* and repulsive interaction must be cause for the correlation, and thus the ordering. However, we have to distinguish between the precursor, the reversible PE atoms, and irreversible platinum atoms that are later expelled onto the surface and eventually lead to growth of the nano-islands. Without a repulsive interaction between the latter, the lifted, reversible PE atoms must be the reason for the ordering, even if they fall back in their holes during the reduction and do not (directly) contribute to the deposition flux.

When considering repulsive interactions in general, typically the first thoughts coming into one's mind are electrical fields and local dipole moments. As sketched in Figure 4a, the oxygen(s), indicated in red, lifting one Pt atom and thereby creating a PE atom/site, will introduce an electrical dipole, which has been addressed experimentally as well as theoretically before.[44,45] In addition, it has been shown recently that dipole moments do have a significant effect on the local energy state of a molecule, atom, or complex on the surface under electrochemical conditions, due to the involved surface charge.[46,47]

Another general candidate is the effect of stress/strain that also can lead to repulsive (or attractive) interactions and that form an analogy with electrical dipoles: it is often overlooked that the mathematical description of stress/strain follows the same route as electrical dipole moments resulting in the same general distance relation for the interaction potential and leading to very similar interaction energies, only varying by the different constants, their interpretation, and their magnitudes. Smoluchowski was the first describing that mechanical displacements, like steps, do create an electrical dipole, due to the propagation of the electronic wave function at them.[48] This dipole moment goes hand in hand with atomic displacements at the step that penetrate also far into the terraces to lower the total free energy. It becomes obvious that a second step or even a single, mechanical "distortion", like an adatom or a vacancy in the terrace, will interact with the stray field of the first step, thereby making the origin indistinguishable, being it

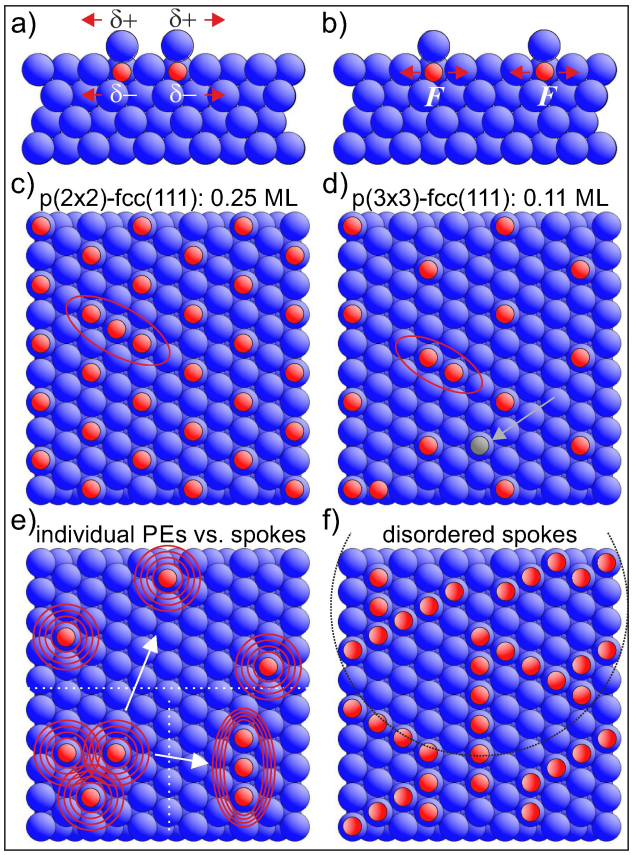

Figure 4. PE atoms and their structures during the reversible PE formation: sketch of the electrical dipole interaction (a) and the stress dipole interaction (b). Note that opposite types of displacements are facing each other in (b) allowing strictly speaking also for attractive interaction. c), d) Superstructures and their critical coverages that should build up with some mobility of the PE atoms: c) with 0.25 ML not one single additional PE atom could be lifted without forming a 1D row or spoke of 3 PE atoms, while in (d) at 0.11 ML there is only one position in the unit cell (see arrow) where one would not create a 1D dimer spoke. e) The energy penalty of 3 closely located PE atoms is significantly larger than 3 PE atoms far apart from each other. However, arranging them in a 1D spoke would be the lowest energy configuration. With attractive interactions 1D spokes would be preferred directly. f) Disordered spokes forming triangular cells and thus preferential nucleation sites. Six closely connected triangles do form one spoke wheel indicated with the dotted circle. Please note that for reasons of visibility, we indicated the oxygen atoms by red balls sitting on top in (c)–(f) instead of drawing them underneath the platinum surface/atoms corresponding to the place exchange (PE).

mechanical or electrical. In the framework of continuum elasticity theory,[49–51] this leads to the well-known step-step-interactions,[52–54] in which the atoms are displaced (from their original positions) in between the steps or sources leading to a strain field that lowers the total surface free energy. Due to the existence of both perpendicular and horizontal dipole/stress moments, the same type of steps (down-down or up-up) always repel each other, whereas the interaction might be attractive or repulsive for opposite type of steps (up-down or down-up). The interaction energy of crossing steps has been treated in Refs. [55,56]. To honor its origin, one also speaks of *Smoluchowski relaxations* covering all type of interactions that can be described with this formalism.

Coming back to our precursor, the reversible PE atoms, and considering the above by recalling that Pt(111) exhibits a huge surface stress being at the verge of reconstructions,[57] that can be triggered with only a small density of adatom or vacancy islands, or even single vacancies,[58–65] one realizes that a PE-site sets up a significant stress field into the terrace, as sketched in Figure 4b. As all PE-sites do have exactly the same atomic structure, one expects a repulsive stress interaction between them, see also above. However, depending on the details of the original surface stress, one cannot completely rule out also the possibility of an attractive stress interaction.

As the combined electrical dipole and the stress interaction is very likely repulsive, and as we will see that the PE-sites will form 1D rows even in the repulsive case, we restrict our argumentation from on here to repulsive interaction, noticing that attractive interaction naturally leads to row formation.

The repulsive interaction between PE atoms leads to a deviation from the standard 2D adatom lattice model described by the PE-site formation energy and entropy $k_B T \ln\frac{\Theta}{1-\Theta}$, in which k_B is the Boltzmann factor, T the temperature, and Θ the coverage in ML. The repulsive interaction is captured by adding $w\Theta$ to the chemical potential of the PE layer, in which w is the interaction energy.[4] Considering only dipole-dipole interactions, the change in chemical potential as a function of coverage is proportional to $\Theta^{3/2}$, as the interaction energy scales with the distance r as r^{-3}.

As a consequence, high PE coverages become impossible, as the system locks already at much lower PE coverage into a perfectly well organized 2D structure/overlayer thereby paying entropy, but lowering the interaction energy to decrease the total free energy (and thus the chemical potential), see Figure 4c and d. Considering the balance between interaction energy and entropy, the 2D structure occurs the earlier the larger w is. Although this could, in principle, explain our observations, there is an inherent problem. Two independent X-ray observations show that the PE layer is (structurally) fully reversible and no nucleation of islands takes place up to around 0.16 ML PE coverage.[28,31] Above this critical coverage, we enter the irreversible part of the PE formation, where an additional PE atom exceeds the critical, local stress field and consequently expels a Pt atom (former PE atom) sidewards onto the terrace to lower the total free energy, instead of lifting it only in height. Figure 4c shows that with a coverage of only 0.25 ML of PE atoms, which corresponds to a p(2×2)-fcc(111) structure, not one single, additional PE atom could be lifted without creating a row of 3 PE atoms. Figure 4d shows that also at a lower coverage of only 0.11 ML, which is significantly below the critical coverage for roughening observed in the X-ray measurements, each additional PE atom will (almost) always make a connection to one existing PE atom forming a dimer row, and thus the beginning of a spoke. Only the gray atom indicated in the

unit cell, would not form a dimer. Consequently, with only mild active PE atom diffusion, a p(3×3) or p(2×2) reconstruction should clearly develop during the reversible part of the PE formation, see also Ref. [66], before Pt atoms are pushed on top of the surface, leading eventually to nucleation of the islands in the irreversible part of the PE formation. Such a superstructure would probably have been noticed in SXRD, but surprisingly has not been reported.[26–32,67] Still there is a solution to this apparent dilemma.

In full analogy to step bunching on miscut, low-index surfaces,[68] the accumulation of a few (stress) dipoles into one larger combined structure can, depending on the precise interaction potential, lower the total free energy in comparison to distributed single dipoles, see the structures in Figure 4e while noticing the resulting stress fields. The anisotropy of the stress field (note Poisson's relation and the orientation difference between the horizontal and vertical direction in Figure 4e) naturally favors the accumulation of PE atoms in one particular orientation leading to the formation of 1D rows as predicted in Ref. [33].

However, it is only a matter of the lengths of the 1D rows before entropy wins, such that a turn is favored according to the 3-fold symmetry and thereby building up spoke-wheel like structures.[35] In addition, as 7 PtO_2 distances equal almost exactly 8 Pt(111) distances, the local stress is relaxed, if one platinum atom is pushed out. Without stress, this lengths also favors the introduction of a turn. Depending on the domain-boundary formation energy as well as the stress within the row, these structures arrange in smaller or larger spoke-wheel like patches, or even in a semi-disordered structure governed mainly by single spokes, as sketched in Figure 4f. Please note, as explained in the following, that one comes to the same result even when not considering domain-boundaries or turns in the spokes. Based on the repulsive interaction and entropy arguments, 1D rows will nucleate and grow here and there on the surface at large distances to each other. In the reversible part, where the Pt atoms in these rows hover over their original lattice positions in the terrace, the total surface stress is increased with each additional PE atom and existing rows grow in length as well as new rows nucleate. This leads to a more "random" nucleation of 1D rows that, with increasing density, look like disordered spoke wheels, as they try to maximize their distances to each other. When the *local* surface stress exceeds the critical value, which corresponds to the critical coverage observed,[28,31] the next PE atom will neither extend the length of an existing row nor nucleate a new row. Instead, even when probably formed at the end of an existing row, it will start the irreversible part of the PE growth and thus the roughening: the critical stress/length of this row is reached such that one atom is pushed on top of the surface while the remaining atoms relax mainly laterally along the row direction. Upon reduction, the remaining PE atoms still forming therow, fall back into their original positions, exactly like during the initial oxidation in the reversible part of PE coverage. However, this time, due to the one expelled PE atom, one vacancy as well as one adatom is created.

With this disordered spoke-wheel structure in mind, the peak in the nucleation distance correlation can be explained in two slightly different ways, comparable to diffusion- vs. attachment/detachment-limited processes and thus depending on the diffusivity of Pt adatoms on the surface. In both cases spokes (PE atom rows) will grow during the reversible part of the PE formation. At a certain length the irreversible part of the PE is locally reached and instead of growing further the PE atom row (spoke) pushes the next Pt atom out as adatom onto the surface. We know that this expelled adatom is oxidized.[26,36] This lowers not only significantly the stress within the row, but favors also the introduction of a kink/corner, where the row changes direction. With limited Pt adatom diffusion the creation of one or more additional Pt adatoms in the vicinity is limiting, as the first atom needs at least a second Pt adatom from a neighboring spoke to form a dimer, if this represents the critical, stable nucleus size. The nucleation in the triangle depends on the number of adatoms created in this vicinity. Not unlikely, the length scale would be increased further, if a trimer would be required for the formation of the critical nucleus describing also a magical cluster.[69] Note that only 1.5 Pt adatoms are created per unit cell of one spoke-wheel triangle.[33,35] Note also that the diameter of one spoke wheel is 4.4 nm and that three triangle bases equal 6.6 nm, which is close to the observed island-island distance of 7.7 nm. The second hypothetical possibility occurs when oxidized Pt adatoms can easily diffuse over long distances on the bare Pt(111) surface. However, the spokes hinder their diffusion, as the diffusion barrier for these PtO_2 adatoms *over* a spoke (PE atom row) is surely significantly increased (making this path maybe even impossible and allowing escape only at the disordered corners). Consequently, the triangular-like areas formed between the individual, disordered spokes, see Figure 4f, serve as nucleation centers, as the lingering time of the adatoms is increased in this way. This time the creation is not the limiting effect, but the restricted diffusion due to the presence of the spokes! Although fundamental different, both scenarios effectively lead to preferential nucleation sites with a certain distance to each other that depends on the favored row/spoke lengths and the degree of disorder.[33]

From a recent study we know that the expelled platinum atoms in the irreversible part of the oxidation, are both oxidized and orders of magnitude slower in diffusion than the bare platinum atoms.[36] Moreover, it also became clear that the expelled platinum atoms, which amounts to about 0.025 ML per ORC,[21] cannot exceed the equilibrium adatom background pressure on the surface to trigger nucleation during the oxidation state.[36] Therefore the real nucleation takes place during the reduction and the ordering comes from the pre-ordering of the expelled atoms in between the row, or spoke-wheel type, structures.[36]

Figure 5 provides a schematic overview of the individual stages of the (pre)oxidation stages leading eventually to the formation of adatom and vacancy islands. At low potentials, <0.95 V and probably starting already around 0.90 V,[31] individual PE atoms are formed that behave like an adatom gas, due to their repulsive dipole interaction. With increas-

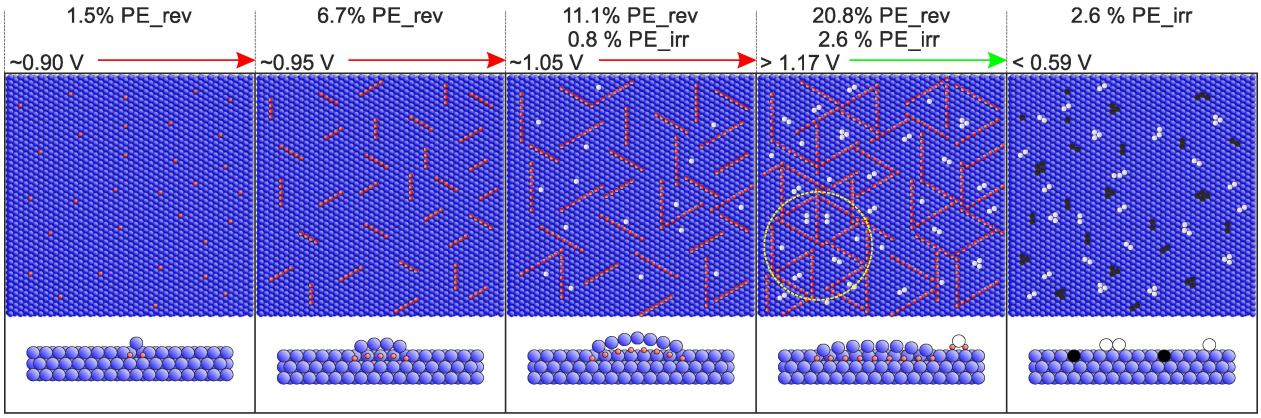

Figure 5. Schematic overview of the individual (pre)oxidation stages leading to the formation of adatom and vacancy islands. Please see the main text for a detailed description and evolution of the individual phases. The images are representative for a particular stage in the evolution somewhere between the indicated voltages, see the upper left corners displayed vs. RHE. Above each image, we indicated the percentage of created reversible PE atoms (PE_{rev}) as well as the percentage of created irreversible PE, thus PtO_2 adatoms (PE_{irr}). These coverages are estimated from the charges in our, as well as others, ORC measurements.[70] Note that 20.8% of PE_{rev} coverage is slightly beyond the reported critical coverage of around 17%, the reason of which depends on the drawn degree of order of the spoke (wheels).[28,31] The created 2.6% of PtO_2 adatoms, however, nicely fits with the reported flux per cycle.[21]

ing coverage, above 0.95 V, the increased energy penalty, due to the repulsive interaction and even shorter distance between the PE atoms, is decreased by assembling the PE atoms into rows instead of keeping an adatom gas. These rows are assembled by PtO_2 units that have a larger lattice constant than the bare Pt surface. As a consequence, these rows buckle in height and push at their ends into the flat surface enhancing the surface stress particular in this direction. At around 1.05 V the row lengths of the reversible PE atoms has reached, for a few rows, the critical lengths/stress such that the first irreversible Pt atoms are pushed onto the surface, where they also get oxidized because of the chemical potential that is in oxidizing conditions. Beyond the reversible PE-peak, around 1.17 V, it is difficult to create more reversible PE atoms.[36] Almost all rows have reached their critical lengths and form together a network structure of triangles or even disordered spoke wheels, as is indicated with the white circle in the image. Each row has pushed out an irreversible Pt atom thereby decreasing the surface stress and thus also the row buckling. Further oxidation at higher potentials, and thus driving forces, will lead to more irreversible Pt atoms and real surface- or even bulk-oxidation.[36] Although small (predominantly dimer) adatom islands are formed during the oxidation, their sizes stay smaller than the critical nucleus size required for the nucleation event under these oxidation conditions.[36] Therefore, technically speaking, the real nucleation occurs during the reduction, although a Pt-dimer adatom island might form a stable nucleus without oxygen (thus low potentials). First the spokes are reduced and the reversible PE atoms fall back into their vacancies.[36] However, as each row pushed out one irreversible Pt atom, one single vacancy is created per reduced row. Below 0.59 V also the irreversible PtO_2 adatoms are reduced allowing them to diffuse again.[36] The formation of the hexagonal pattern is a consequence of the formation of the network structure by the spokes that assemble in triangles of even disordered spoke wheels. The dimers captured in these triangles very likely form the stable nuclei upon reduction. Otherwise, the hexagonal pattern evolves during the diffusion after the spokes are reduced, as the random walks start on well, pre-defined positions imprinted by the rows.

Interestingly, the measurable peak in the nucleation-distance correlation, which indicates the existence of either repulsive interaction or preferential nucleation sites, is introduced by preferential nucleation sites that *a priori* do not exist and are created by a precursor, the reversible PE atoms, during the early stages of the oxidation.

3. Conclusion

In conclusion, we have statistically analyzed our electrochemical roughening data on Pt(111) during oxidation-reduction cycles measured with an Electrochemical Scanning Tunneling Microscope with the isotropic pair correlation function to extract the island-island distance distribution during the nucleation and also somewhat later stages. The distance distribution function clearly shows a peak, which proves the existence of a repulsive interaction or pre-defined, preferential nuclei sites. As the peak becomes visible already from on cycle #5 at only 80% of the fully nucleation density that is reached significantly later at cycle #9, the interaction or order of preferential sites has to be rather strong. It is interesting to note that the peak height still increases even after the full nucleation density has been reached. As the growth is determined by the Zeno growth-instability, mild material transport between neighboring islands based on downhill funneling leads to the development of more equally shaped islands with increasing height. As the precursor for island nucleation is given by the creation of place-exchanged (PE) atoms that repel each

other, one might think that this is the reason for the correlation in the nucleation. However, island nucleation does not occur in the first, reversible part of the PE atom creation, which is up to around 0.17 ML. At this coverage not one single additional PE atom could be lifted without connecting to existing ones thereby forming rows leading to spokes. Moreover, with the repulsive interaction a $p(2\times2)$ or $p(3\times3)$ structure is expected, which has not been observed experimentally. Stress and free energy arguments point towards the formation of 1D PE atom rows, and thus spokes, during the reversible part of the PE. At the critical coverage, when the local critical stress is reached around 0.17 ML, a row pushes one atom onto the terrace instead of growing further thereby relaxing the stress and lowering the chemical potential. This happens during the irreversible part of the PE formation leading eventually to the nucleation of islands. As the rows will follow the 3 fold symmetry, (disordered) spoke-wheel like structures are expected to form, similar to the ones reported earlier. The atom rows, the spokes, and in particular their lengths is the reason for the correlated nucleation at preferential nucleation sites. Atoms are pushed out into the triangular like patches during the irreversible part of the oxidation, but the real nucleation happens during the reduction, as the flux of expelled atoms cannot exceed the equilibrium adatom density during oxidation required for nucleation. Some fine details, like the row/spoke lengths has been addressed earlier.[33] However, the optimum length in combination with the degree of disorder of the spoke wheels, depends on the dipole-moment magnitude of the PE atoms, the surface charge, and the surface stress/strain. These aspects are beyond the current manuscript and are subject for future studies. Theoretical groups could play an important role here, see Ref. [46].

Fundamentally, it is interesting to notice that the origin of the peak in the nucleation-distance correlation is given by nucleation at preferential sites that did not exist before (instead of a direct repulsive interaction between the depositing Pt atoms), whereas these sites, the triangles between the rows, are created during the early stages during the oxidation by a repulsive interaction of the precursor, the reversible PE atoms.

Indications exist that the nucleation at preferential sites that do not exist *a priori*, and are created during the early stages of the evolution (chemical reaction), is a rather general mechanism: many other surfaces, like copper, silver, and gold, show the formation of similar nano-islands upon repeated oxide formation and reduction.[71–74] We expect similar effects to occur also for nitride and sulfide formation. All of them create dipole moments during the reaction, in which a new surface structure is formed with a larger lattice constant. This creates surface stress that, in a later stage, eventually expels atoms.

Finally, as the prevention of the nucleation is the most effective way for preventing the roughening and thus electrode degradation, the above insights pave the way for directed research focused on the inhibition of the nucleation.

Acknowledgements

M. J. Rost acknowledges fruitful discussions with Francesc Valls Mascaro and J. Bjarke V. Mygind on the structure, existence and ordering of the "spoke wheel" like structures. The authors acknowledge LVH Coatings for supplying their Clearclad electrophoretic paint. The authors acknowledge financial support from the Dutch Organizaton of Scientific Research (NWO) via the TOP-project with number: 716.017.001.

Conflict of Interest

The authors declare no conflict of interest.

Data Availability Statement

The data that support the findings of this study are available from the corresponding author upon reasonable request.

Keywords: Electrochemistry · Non-Random Nucleation · Oxidation-Reduction Cycles · Place Exchange · Platinum

[1] H. Brune in *Epitaxial Growth of Thin Films in Surface and Interface Science: Solid-Solid Interfaces and Thin Films*, 1st ed. (Ed.: Wandelt), Wiley-VCH, Weinheim, **2014**, p. 421.
[2] A. Milchev, *Electrocrystallization: Fundamentals of Nucleation and Growth*, Springer, Heidelberg, **2002**.
[3] J. A. Venables, *Introduction to Surface and Thin Film Processes*, Cambridge University Press, Cambridge, **2000**.
[4] H. Ibach, *Physics of Surfaces and Interfaces*, Springer, Heidelberg, **2006**.
[5] W. K. Burton, N. Cabrera, F. C. Frank, *Philos. Trans. R. Soc. London* **1951**, *243*, 299.
[6] F. Meissner, *Z. Anorg. Allg. Chem.* **1920**, *110*, 169.
[7] E. Rie, *Z. Phys. Chem.* **1920**, *57*, 137; E. Rie, *Z. Phys. Chem.* **1923**, *104*, 354.
[8] D. D. Chambliss, R. J. Wilson, S. Chiang, *Phys. Rev. Lett.* **1991**, *66*, 1721.
[9] G. Rosenfeld, K. Morgenstern, M. Esser, G. Comsa, *Appl. Phys. A* **1999**, *69*, 489.
[10] K. Morgenstern, *Phys. Status Solidi B* **2005**, *242*, 773.
[11] B. Lewis, D. S. Campbell, *J. Vac. Sci. Technol.* **1967**, *4*, 209.
[12] J. A. Venables, *Philos. Mag.* **1973**, *27*, 697.
[13] J. J. Metois, J. C. Zanghi, R. Kern, *Philos. Mag.* **1976**, *33*, 133.
[14] J. L. Robins, T. N. Rhodin, *Surf. Sci.* **1964**, *2*, 346.
[15] P. W. Palmberg, P. W. Todd, T. N. Rhodin, *J. Appl. Phys.* **1968**, *39*, 4650.
[16] H. Bethge, *J. Vac. Sci. Technol.* **1969**, *6*, 460.
[17] A. D. Henning, J. S. Vermaak, *Philos. Mag.* **1970**, *22*, 281.
[18] J. W. Evans, P. A. Thiel, M. C. Bartelt, *Surf. Sci. Rep.* **2006**, *61*, 1.
[19] L. Jacobse, Y.-F. Huang, M. T. M. Koper, M. J. Rost, *Nat. Mater.* **2018**, *17*, 277.
[20] D. J. S. Sandbeck, O. Brummel, K. J. J. Mayrhofer, J. Libuda, I. Katsounaros, S. Cherevko, *ChemPhysChem* **2019**, *20*, 2997.
[21] M. J. Rost, *J. Electrochem. Soc.* **2023**, *170*, 012504.
[22] H.-J. Ernst, et al., *Phys. Rev. Lett.* **1994**, *72*, 112.
[23] M. Giesen, G. Schulze Icking-Konert, H. Ibach, *Phys. Rev. Lett.* **1999**, *82*, 3101.

[24] M. A. H. Lanyon, B. M. W. Trapnell, *Proc. R. Soc. London Ser. A* **1955**, *227*, 387.
[25] K. J. Vetter, J. W. Schultze, *J. Electroanal. Chem.* **1972**, *34*, 141.
[26] L. Jacobse, V. Vonk, I. T. Mc Crumb, C. Seitz, M. T. M. Koper, M. J. Rost, A. Stierle, *Electrochim. Acta* **2022**, *407*, 139881.
[27] J. Drnec, M. Ruge, F. Reikowski, B. Rahn, F. Carlà, R. Felici, J. Stettner, O. M. Magnussen, D. A. Harrington, *Electrochim. Acta* **2017**, *224*, 220.
[28] J. Drnec, M. Ruge, F. Reikowski, B. Rahn, F. Carlà, R. Felici, J. Stettner, O. M. Magnussen, D. A. Harrington, *Electrochem. Commun.* **2017**, *84*, 50.
[29] M. Ruge, J. Drnec, B. Rahn, F. Reikowski, D. A. Harrington, F. Carlà, R. Felici, J. Stettner, O. M. Magnussen, *J. Electrochem. Soc.* **2017**, *164*, H608.
[30] M. Ruge, J. Drnec, B. Rahn, F. Reikowski, D. A. Harrington, F. Carlà, R. Felici, J. Stettner, O. M. Magnussen, *J. Am. Chem. Soc.* **2017**, *139*, 4532.
[31] H. You, D. J. Zurawski, Z. Nagy, R. M. Yonco, *J. Chem. Phys.* **1994**, *100*, 4699.
[32] Y. Liu, A. Barbour, V. Komanicky, H. You, *J. Phys. Chem. C* **2016**, *120*, 16174.
[33] S. Hanselman, I. T. McCrum, M. J. Rost, M. T. M. Koper, *Phys. Chem. Chem. Phys.* **2020**, *22*, 10634.
[34] D. Boden, I. M. N. Groot, J. Meyer, *Phys. Chem. Chem. Phys.* **2022**, *126*, 20020.
[35] M. A. van Spronsen, J. W. M. Frenken, I. M. N. Groot, *Nat. Commun.* **2017**, *8*, 429.
[36] F. Valls Mascaró, I. T. McCrum, M. T. M. Koper, M. J. Rost, *J. Electrochem. Soc.* **2022**, *169*, 112506.
[37] L. Jacobse, M. J. Rost, M. T. M. Koper, *ACS Cent. Sci.* **2019**, *5*, 1920.
[38] K. Itaya, S. Sugawara, K. Sashikata, N. Furuya, *J. Vac. Sci. Technol. A* **1990**, *8*, 515.
[39] K. Sashikata, N. Furuya, K. Itaya, *J. Electroanal. Chem.* **1991**, *316*, 361.
[40] https://www.youtube.com/watch?v=xSpRcsgxq3Q.
[41] M. Giesen, H. Ibach, *Surf. Sci. Lett.* **2000**, *464*, L697.
[42] M. J. Rost, *Phys. Rev. Lett.* **2007**, *99*, 266101.
[43] D. M. Kolb, *Prog. Surf. Sci.* **1996**, *51*, 109.
[44] Y. Furuya, T. Mashio, A. Ohma, N. Dale, K. Oshihara, G. Jerkiewicz, *J. Chem. Phys.* **2014**, *141*, 164705.
[45] M. J. Eslamibidgoli, M. H. Eikerling, *Electrocatalysis* **2016**, *7*, 345.
[46] S. D. Beinlich, N. G. Hörmann, K. Reuter, *ACS Catal.* **2022**, *12*, 6143.
[47] A. M. Dudzinski, E. Diesen, H. Heenen, V. J. Bukas, K. Reuter, *in preparation*.
[48] R. Smoluchowski, *Phys. Rev.* **1941**, *60*, 661.
[49] L. D. Landau, E. M. Lifschitz, *Theory Of Elasticity, Vol. 7*, Pergamon, Oxford, **1959**.
[50] K. H. Lau, W. Kohn, *Surf. Sci.* **1977**, *65*, 607.
[51] V. I. Marchenko, A. Ya Parashin, *Sov. Phys. JETP* **1980**, *52*, 129.
[52] P. Nozières in *Solids Far From Equilibrium* (Ed.: C. Godrèche), Cambridge University Press, Cambridge, **1992**, p. 1.
[53] J. Lapujoulade, *Surf. Sci. Rep.* **1994**, *20*, 191.
[54] L. E. Shilkrot, D. J. Srolovitz, *Phys. Rev. B* **1996**, *53*, 11120.
[55] M. J. Rost, S. B. van Albada, J. W. M. Frenken, *Europhys. Lett.* **2002**, *59*, 559.
[56] M. J. Rost, S. B. van Albada, J. W. M. Frenken, *Surf. Sci.* **2003**, *547*, 71.
[57] R. J. Needs, M. J. Godfrey, M. Mansfield, *Surf. Sci.* **1991**, *242*, 215.
[58] M. Bott, M. Hohage, T. Michely, G. Comsa, *Phys. Rev. Lett.* **1993**, *70*, 1489.
[59] M. Hohage, T. Michely, G. Comsa, *Surf. Sci.* **1995**, *337*, 249.
[60] C. Teichert, M. Hohage, T. Michely, G. Comsa, *Phys. Rev. Lett.* **1988**, *72*, 1682.
[61] A. R. Sandy, S. G. J. Mochrie, D. M. Zehner, G. Grübel, K. G. Huang, D. Gibbs, *Phys. Rev. Lett.* **1992**, *68*, 2192.
[62] P. Grütter, U. T. Dürig, *Phys. Rev. B* **1994**, *49*, 2021.
[63] P. Grütter, U. T. Dürig, *Surf. Sci.* **1995**, *337*, 147.
[64] Z. Lanping, J. Ek, U. Diebold, *Phys. Rev. B* **1998**, *57*, R4285.
[65] B. Holst, M. Nohlen, K. Wandelt, W. Allison, *Phys. Rev. B* **1998**, *58*, R10195.
[66] J. M. Hawkins, J. F. Weaver, A. Asthagiri, *Phys. Rev. B* **2009**, *79*, 125434.
[67] C. Ellinger, A. Stierle, I. K. Robinson, A. Nefedov, H. Dosch, *J. Phys. Condens. Matter* **2008**, *20*, 184013.
[68] H.-C. Jeong, E. D. Williams, *Surf. Sci. Rep.* **1999**, *34*, 171.
[69] S. C. Wang, G. Ehrlich, *Surf. Sci.* **1990**, *239*, 301.
[70] A. M. Gómez-Marín, J. M. Feliu, *Electrochim. Acta* **2012**, *82*, 558.
[71] C. Köntje, D. M. Kolb, G. Jerkiewicz, *Langmuir* **2013**, *29*, 10272.
[72] N. Furuya, M. Ichinose, M. Shibata, *J. Electroanal. Chem.* **1999**, *460*, 251.
[73] Y. Grunder, J. Beane, A. Kolodziej, C. A. Lucas, P. Rodriguez, *Surfaces* **2019**, *2*, 145.
[74] D. D. Tuschel, J. E. Pemberton, J. E. Cook, *Langmuir* **1986**, *2*, 380.

Manuscript received: November 7, 2022
Accepted manuscript online: February 23, 2023
Version of record online: May 23, 2023